#3590 INSTITUTE OF PAPER CHEMIS'
(Fiber Orientation Measuremen
Project Reports (2

PROJECT REPORT FORM

Project No. 3590
Cooperator Institute exploratory
Report No. 5
Date January 26, 1987
Signed [signature]

Preliminary experiments on measuring light scattering power of fiber suspensions.

A flow-through channel, as sketched in Figure 1, was employed in a pump around flow loop. The fiber suspension was thoroughly dispersed in the channel section providing three windows; A, B, and C. Incandescent light was directed through window, A, and the transmitted light intensity, T, was measured through window B. The intensity of scattered light was measured through window C.

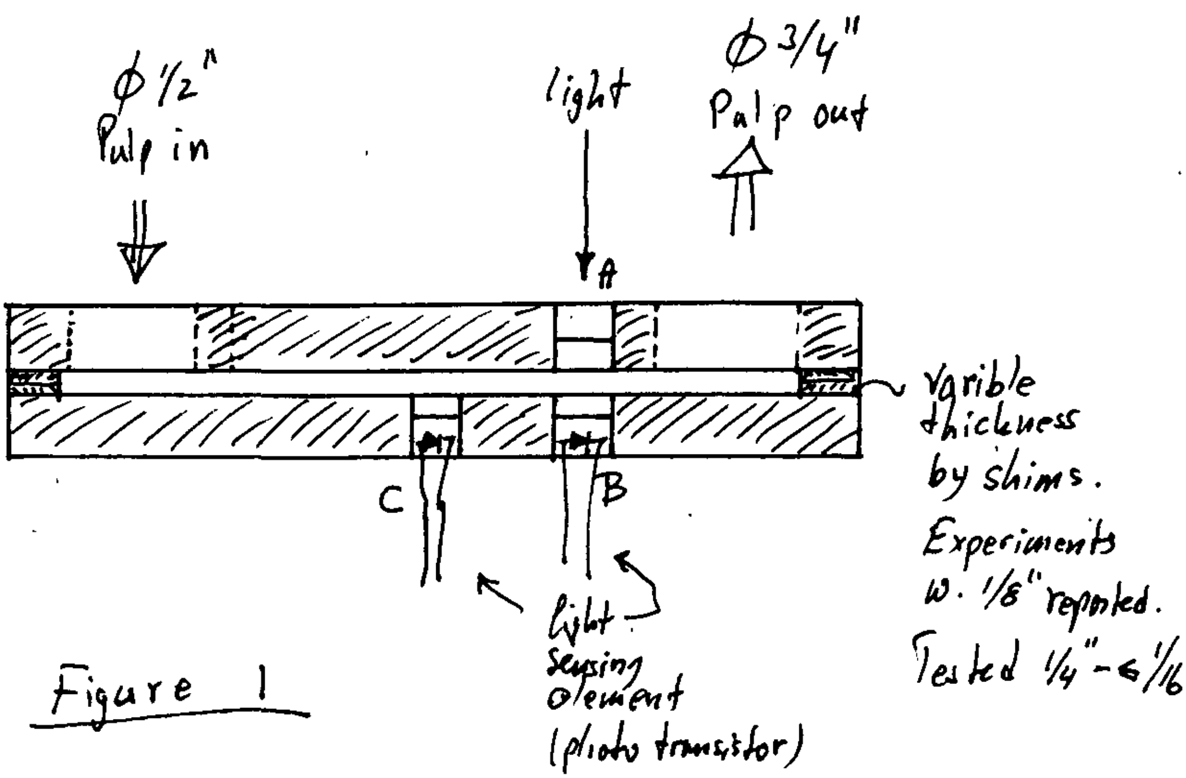

Figure 1

The idea was that, as the light scattering power of the suspension increases, two things happen. First, the intensity of the transmitted light will decrease and the intensity of the scattered light, S, measured through window C, will increase at low consistencies and then decrease. The ratio S/T should be a measure of the light scattering power of the suspension. The following pages give an excerpt of results obtained in a preliminary run. A number of runs were made with similar results but, due to the pump employed, consistency was limited to about 2%.

This system should be combined with a measure of R_∞. Together, the two measurements should make it possible to evaluate the specific light scattering properties. A crude device to measure R_∞ was constructed and was found to work reasonably well. However, it required a very thick channel or tank for ideal operation. A few experiments were run in a five gallon bucket and, at consistencies above 1%, reflectivity was found to be independent of consistency.

Due to the demands from a member company during research and development in the same area, the project was shelved in mid-1984 and was never restarted. The complete flow channel was left to Gary Baum. It was placed on the table containing the apparatus with the rotating polarizers.

From a seminar on Number Commander. 16

SUSP OPTICS

THESE ARE THE NUMBERS, PLOTTING SYMBOLS AND NAMES OF THE VARIABLES:

1. ---	1 --	TIME	2. ---	2 --	DRIVER VOLTS
3. ---	3 --	SCATT.VOLTS	4. ---	4 --	TRANSM.VOLTS
5. ---	5 --	S/T RATIO	6. ---	6 --	MOTOR V.
7. ---	7 --	PRESSURE PSI	8. ---	8 --	RUNTIME
9. ---	9 --	CONC. G/L	10. ---	A --	CUPS ADDED
11. ---	B --	OPEN FILE 1	12. ---	C --	OPEN FILE 2
13. ---	D --	OPEN FILE 3	14. ---	E --	FLAG

There are sets numbered up to 38 on the disk.

Exploration of an optical method to characterize pulp suspensions; an account of one day of experimentation.

The following few pages serve as an example of how Number Com mander® can be used to evaluate data from a small investigation. Data are kept in a file named "Susp Optics". The table above was printed out with the "Make Tables" program, option "C". An electronic setup was used in which the sensitivity of the system was governed by the voltage to the driver circuit. Light transmission and light scattering were measured. The rate of flow was controlled by the voltage to the pump motor. The total pressure in the measurement cell was varied at three different levels. The time was noted for each experiment. The series of expriments extended from 11:00 AM through 3:00 PM (1500). I took a break to do some real work and for lunch, between 11:30 AM and 1:30 PM. In the meantime, the suspension was just sitting in the open vessel. The parameter RUN TIME excludes any and all periods of time when the suspension was not being circulated.

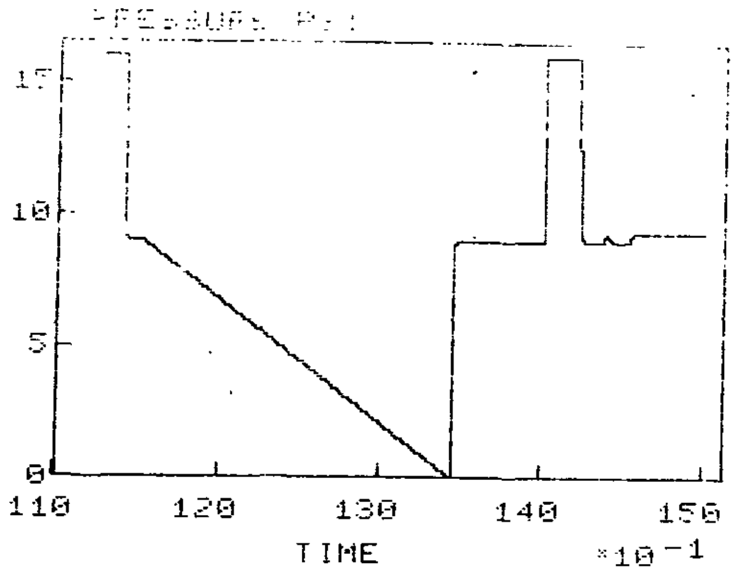

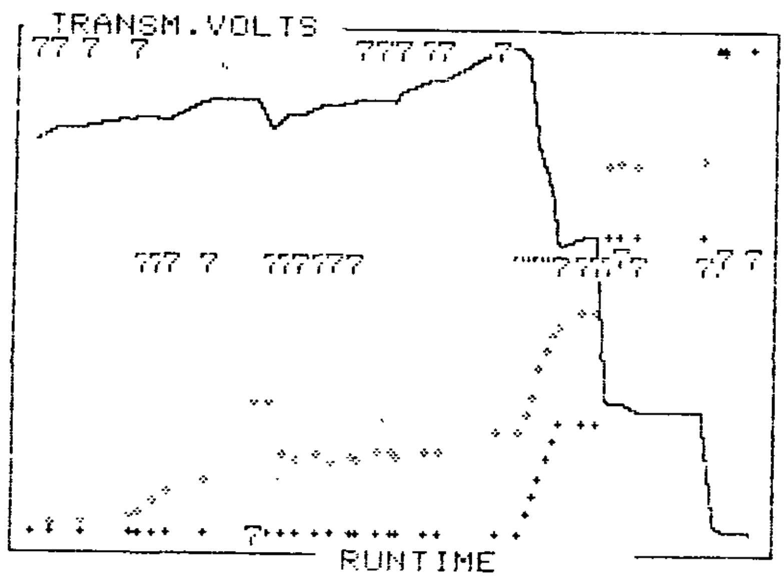

OVERVIEW OF OPERATIONS

1. The pressure in the system was varied according to the schedule in the upper diagram.

2. The lower plot was auto-scaled for several of the important parameters and the plots superimposed. The first part of the experiment was designed to investigate the stability of the system under various operating conditions and using a constant concentration of fibers. The second part of the experiment, started at about 1:30 PM, was designed to investigate the sensitivity of the system to consistency variations. Consistency was varied by adding pulp to the system in increments of one cup of concentrated pulp.

Fully drawn line = light transmission signal
Diamonds = light scattering signal
7 = system pressure
+ = cups of pulp added to the system

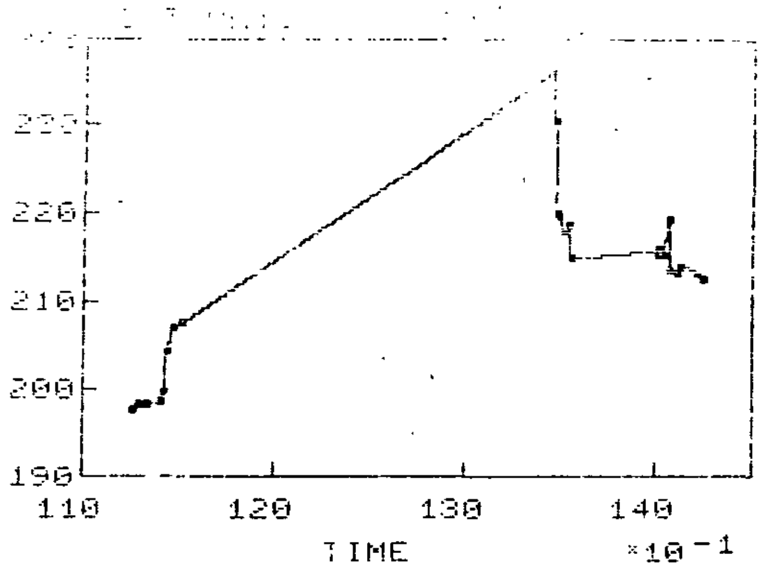

3. The ratio of light scattering to transmission (S/T) is shown as a function of time at constant concentration of fibers. It appears that when the suspension was allowed to sit in the tank without pressurization, the S/T ratio increased, probably due to the presence of air.

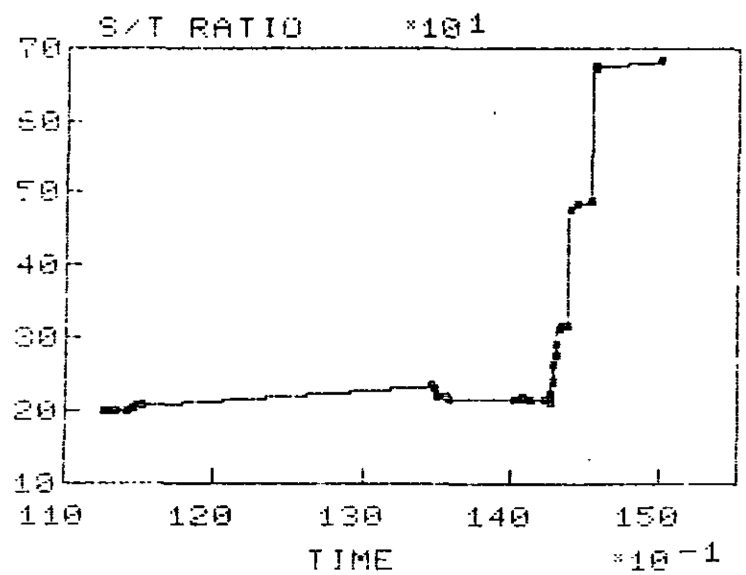

4. The S/T variations noted above are small, however, compared to the ones introduced by the addition of pulp.

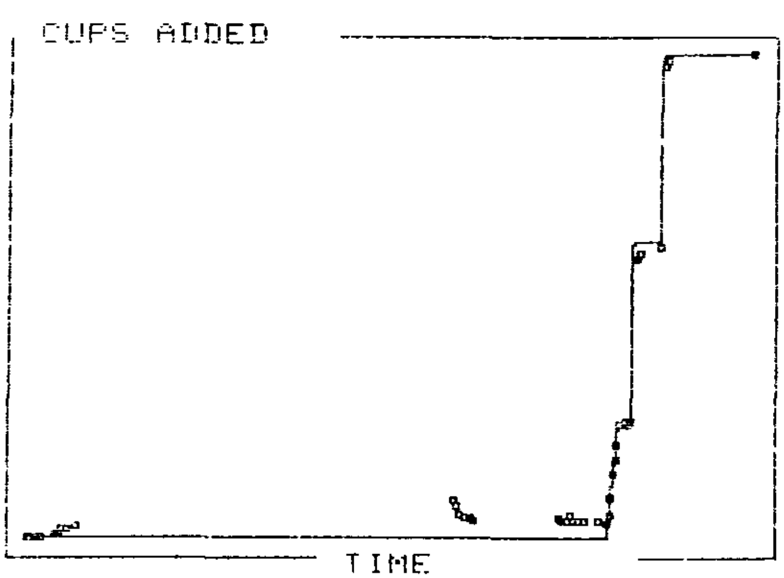

5. This is an auto-scaled diagram showing two parameters. The fully drawn line represents the number of cups added and the squares represent the S/T ratio. It appears that, apart from the variation introduced by the long break, there should be a good correlation between the number of cups added and the S/T ratio.

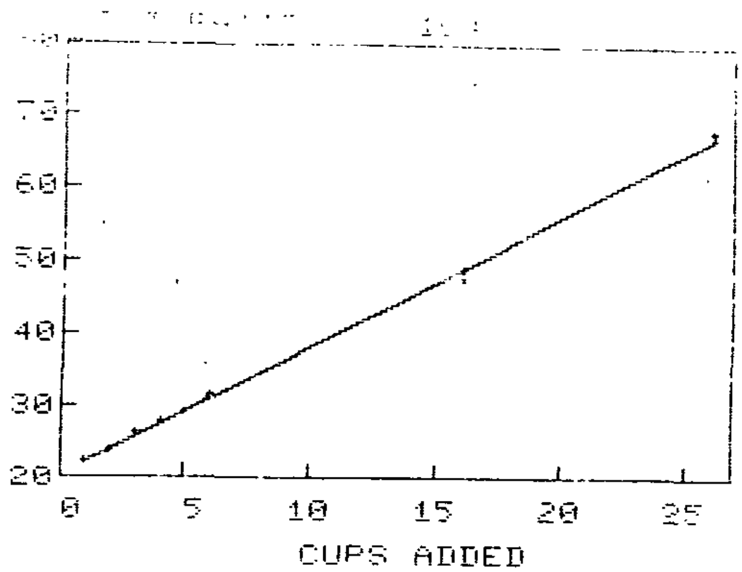

FILE: SUSP OPTICS. IPC - DOUGLAS WAHREN 10/2/84

VERTICAL: 5 = S/T RATIO : 2 to 8
HORIZONTAL: CUPS ADDED : 0 to 26.78
Set #: 24 to 38.
Number of points inside diagram, used for regression analysis (if any), = 15.
Coefficient of Determination, R^2 = .998263635
Correlation Coefficient, R = 99.9131441 %.
Calculated Regression Equation:
S/T RATIO = 2.02756135 + (.179620456) * (CUPS ADDED)
Standard Error of Estimate of S/T RATIO = .071169687

6. As expected, there is a strong correlation between the number of cups added and the S/T ratio. Note that in order to avoid "loading" the correlation at one end with meaningless data, I have only used data sets numbered 24-38, i.e., the ones where cups of pulp were added. The correlation coefficient is shown to be 99.9%. The calculated regression equation is printed out using the names of variables. A standard error of estimate is given, too.

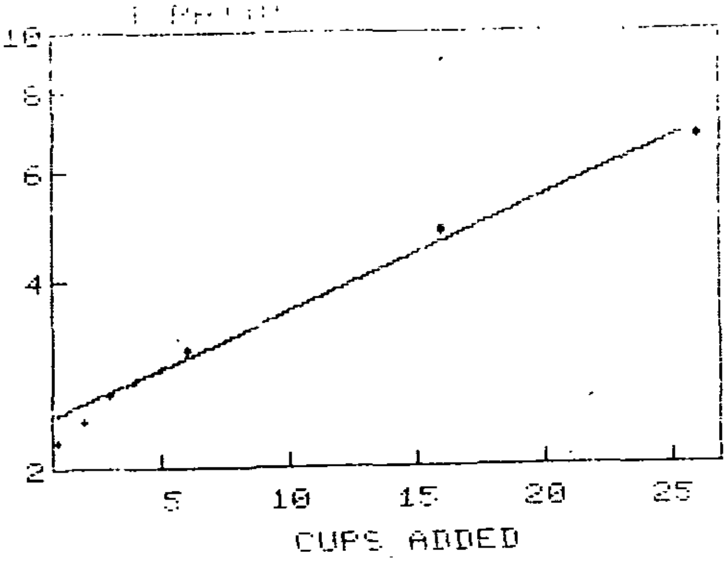

FILE: SUSP OPTICS. IPC - DOUGLAS WAHREN 10/2/84

VERTICAL: 5 = S/T RATIO , LOG-SCALE: 2 to 10
HORIZONTAL: CUPS ADDED : .700000001 to 26.78
Set #: 24 to 38.
Number of points inside diagram, used for regression analysis (if any), = 15.
Coefficient of Determination, R^2 = .985615561
Correlation Coefficient, R = 99.2781729 %.
Calculated Regression Equation:
S/T RATIO = (2.33769711) * (1.04335103) ^ (CUPS ADDED)
Standard Error of Estimate of S/T RATIO = 4.75390033 %

7. Replotting the same data on log/log and semi/logarithmic scales brought no improvement of the good correlation shown in the previous diagram.

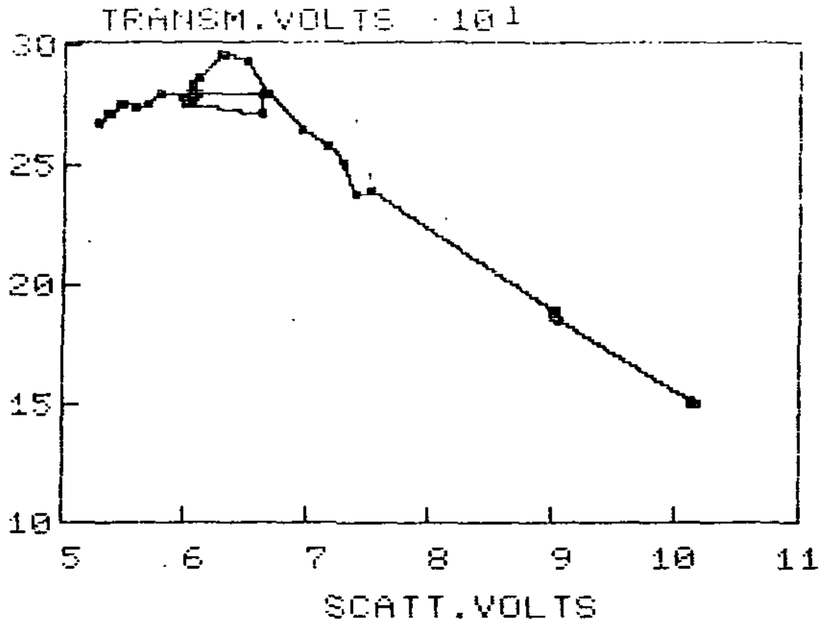

8. This diagram shows all data on light transmission and light scattering. It is presented here to prove that there is no unique dependence between these two variables. Their relationship is influenced by pressure, running time in the system and probably other variables in addition to the concentration of fibers.

PROJECT REPORT FORM

Project No. 3590
Cooperator Institute exploratory
Report No. 4
Date January 19, 1987
Signed [signature]

Setting the Jet - Part 1: Roll-Type Twin Wire Formers

SETTING THE JET - PART 1: ROLL-TYPE TWIN WIRE FORMERS

D. Wahren
The Institute of Paper Chemistry*
Appleton, WI 54912

ABSTRACT

Twin wire formers of the roll type have the potential to provide high capacity, high retention and complete control of fiber orientation (1,2). In addition, they are also well suited for simultaneous multilayer forming processes (3). In order to gain full control of fiber orientation and to attain maximum purity of individual layers in multilayer forming operations, it is necessary to pay close attention to the correct setting and velocity of the jet. The following is a quantitative treatment of the subject based on a portion of material presented at the 1980 Pacific TAPPI Seminar (4).

GENERAL PROCEDURE

The general procedure is as follows.

First, determine the requirements based on paper grade, machine speed, etc., and deduce the appropriate parameter values at the point (or line) where the jet is to be landed. The main parameters are:

- Jet thickness
- Jet velocity
- Jet angle
- Jet elevation or "dig" into the forming roll.

Second, determine the jet trajectory "backward" from the forming roll to the headbox. This is an application of conventional fluid mechanics, usually simplified to the form of a friction-free, "free fall" parabola.

Third, determine the headbox settings. The actual parameters to be determined vary with headbox design and method of suspension but, in principle, include the following:

- Slice opening
- Location of end of one or both slice lips
- Tilt of headbox and/or slice lips
- *Pressure at location of pressure sensor*

There is considerable interaction between satisfactory settings of these parameters. The Appel equations (5,6) can be used to calculate suitable combinations once the user supplies the basic information. Iterative solution techniques have to be employed but convergence is very rapid (approximately one second or less on a PC).

CONDITION OF THE JET AT THE LANDING POINT

The jet thickness, h, is determined by the required basis weight, W, the effective single-pass retention, N, the desired or required dilution or forming consistency, C, and the jet/wire velocity ratio:

$$W = N \cdot h \cdot C \cdot V_j/V_w \tag{1}$$

*Present address: STORA Technology, S-79180 Falun, Sweden

Note that, for this particular calculation, it does not matter where along the jet trajectory the jet thickness is calculated - as long as corresponding values of h and V_j are used.

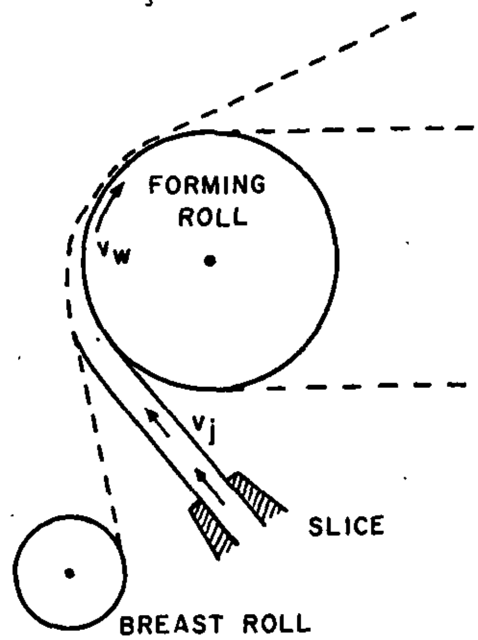

Fig. 1. Twin wire former jet velocity.

The required free jet velocity (V_j, see Fig. 1) depends on the outer wire tension and the forming roll speed, in accordance with the following physical principles. First, it can be shown that the gage pressure in the forming zone is:

$$P_{FZ} = T'/R \tag{2}$$

where: T' = outer wire tension per unit width
R = forming roll radius

Second, the free jet must have sufficient kinetic energy to overcome the forming zone pressure. For a given final suspension velocity (V_{FZ}) in the forming zone, the required free jet approach velocity (V_j) is governed by Bernoulli's equation:

$$\rho \frac{V_{FZ}^2}{2} + P_{FZ} = \rho \frac{V_j^2}{2} \tag{3}$$

where: ρ = density of suspension

Combining this equation with Eq. (1) gives:

$$V_j = \sqrt{V_{FZ} + 2T'/\rho R} \tag{4}$$

For the special case where $V_{FZ} = V_W$ (V_W = forming roll tangential surface velocity) a "square" sheet is formed. The needed jet velocity in this case is:

$$V_j = V_{j_o} = \sqrt{V_w^2 + 2T'/\rho R} \tag{5}$$

where: V_{j_o} = jet velocity needed to form a "square" sheet.

In general, the fiber orientation in the sheet is governed by the differential jet velocity:

$$\Delta V_j = V_j - V_{j_o} \qquad (6)$$

The resulting ratio (TR) of tensile strengths in the machine and cross machine directions for sheets dried freely or fully constrained has been found to be related to ΔV_j by:

$$TR = \left| \frac{\Delta V_j}{U} \right|^b + d \qquad (7)$$

Approximate parameter values for corrugating medium are:

$U = 1$ m/sec
$b = 1.6$
$d = 1.15$

In addition, increased tension during drying raises the tensile ratio. The forming fabric also exerts an influence, particularly on d.

Having selected the free jet velocity entering the forming zone, one must then consider the position and orientation of the jet relative to the forming roll and the breast roll. It is important that the jet be "captured" smoothly by the twin wires in order to avoid splashing, poor formation, etc. Two approaches to selecting the proper jet/roll configuration are described here. In practice, they yield nearly identical results for thin jets.

The simpler method (see Fig. 2) is based on the physically reasonable requirement that the jet should enter the forming zone tangent to both the forming roll and the outer wire.* According to the geometrical relationships shown in Fig. 2:

$$\cos(\sigma_{FZ} - \beta) = ((R + r + h)/(R + r + H)) \qquad (8)$$

or,

$$\sigma_{FZ} = \beta + \cos^{-1}((R + r + h)/(R + r + H)) \qquad (9)$$

where:

σ_{FZ} = angle at which jet first contacts forming roll and wire
β = angular position of breast roll with respect to forming roll
h = nominal free jet thickness
H = distance between forming roll and breast roll
r = breast roll radius
R = forming roll radius

To ensure that effects of jet surface ripples, irregularities and consequent air entrainment (potentially detrimental to sheet formation) are minimized, the jet is then moved radially "into" the roll by an amount corresponding to the jet surface irregularities.

The second approach for selecting the geometry of jet entry into the twin wire forming zone is slightly more mathematically complex than the previous one. This method is recommended for thin jets of free stock where the hydraulic forming pressure may not be high enough to deflect the forming fabric significantly. This method is based on the requirement that the jet bisects the angle between the outer wire and the tangent to the forming roll at the point of initial jet contact (see Fig. 3). Thus, this method could be termed "symmetrical jet placement." To ensure that the effects of jet surface ripples, irregularities and consequent air entrainment (potentially detrimental to good sheet formation) are minimized, the jet can, again, be moved radially "into" the forming roll, i.e., the roll can be caused to intercept part of the jet (dimension δ in Fig. 3). For the configuration in Fig. 3, the proper value of the forming zone jet angle (σ_{FZ}) can be found as follows:

First, considering the right triangle inscribed on the forming roll, the Pythagorean theorem dictates that:

$$b^2 = R^2 - (R - \delta)^2 \qquad (10)$$

or,

$$b^2 = \delta(2R - \delta) \qquad (11)$$

Second, considering the same triangle,

$$\sin\phi = \frac{b}{R} \qquad (12)$$

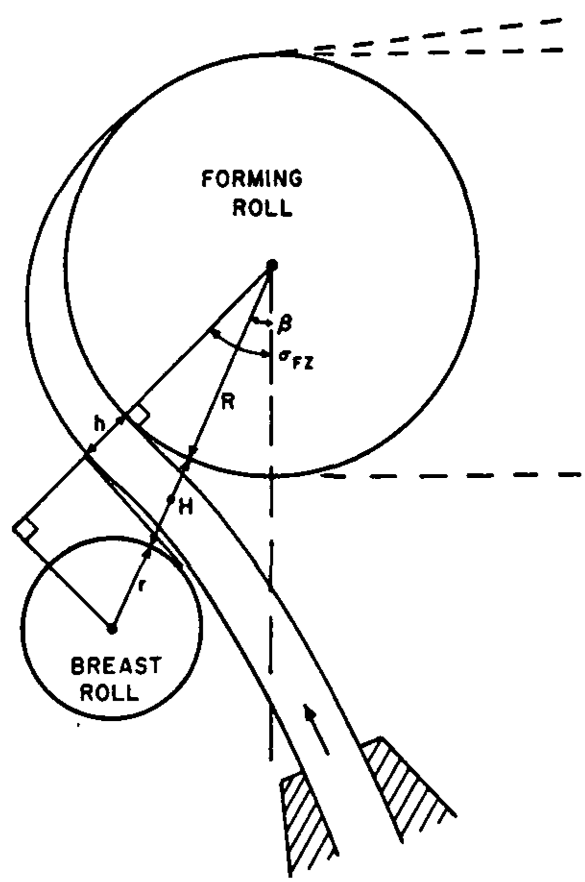

Fig. 2. Forming zone geometry for tangential jet entry.

*In principle, since the jet velocity changes during the process of entering the forming zone [per Eq. (3)], mass conservation dictates that the jet thickness also changes. However, it appears that, for typical parameter values, the change in jet thickness during the entering process is only a few percent. Therefore, only the nominal thickness (h) is considered here.

2

or, using the previous equation:

$$\sin\phi = \sqrt{\frac{\delta}{R}\left(2 - \frac{\delta}{R}\right)} \qquad (13)$$

or,

$$\phi = \sin^{-1}\sqrt{\frac{\delta}{R}\left(2 - \frac{\delta}{R}\right)} \qquad (14)$$

Alternatively, if one considers the small triangle in the forming zone, it can be shown that:

$$\phi = \sin^{-1}\left\{1/\sqrt{1 + 4\delta\,(2R - \delta)/h^2}\right\} \qquad (15)$$

Next, considering the largest right triangle defined in Fig. 3, the angle ψ is given by

$$\psi = \cos^{-1}\left(\frac{R + r}{R + r + H}\right) \qquad (16)$$

Finally, consideration of the geometrical relationships between angles in Fig. 3 shows that:

$$\sigma_{FZ} = \beta + \psi - \phi \qquad (17)$$

Since β is assumed to be a known design parameter, the preceding equations are sufficient to calculate σ_{FZ} as a function of other design parameters and the jet thickness.

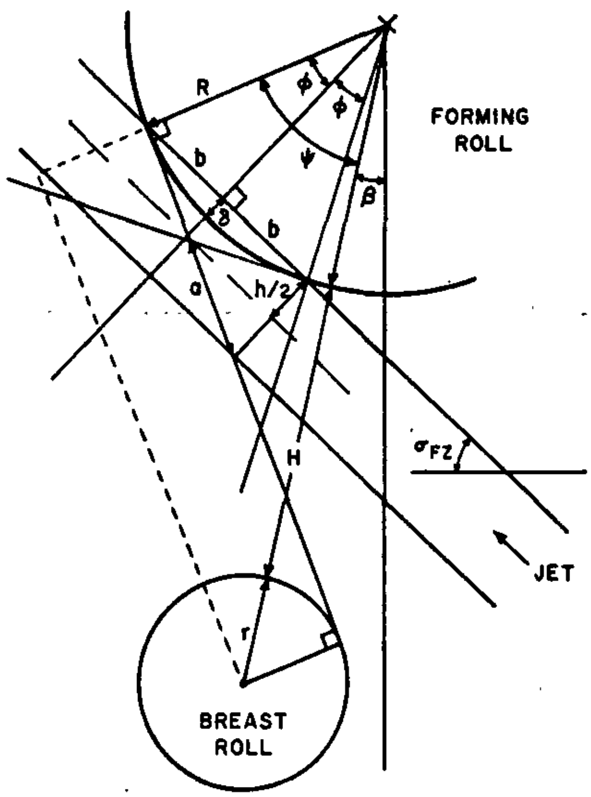

Fig. 3. Symmetrical placement of free jet between forming roll and outer wire.

THE JET TRAJECTORY

Now that the forming zone entrance region has been defined in terms of jet velocity and configuration, the necessary orientation and jet velocity at the slice can be determined. To do so requires consideration of the effects of gravity on the jet as it travels from the slice to the forming roll. The qualitative effects are that the vertical component *of jet velocity decreases as the jet moves upward* (or increases as it moves downward) and consequently, the jet trajectory becomes parabolic rather than linear. These effects are quantified in the following. Parameters in the equations are indicated in Fig. 4.

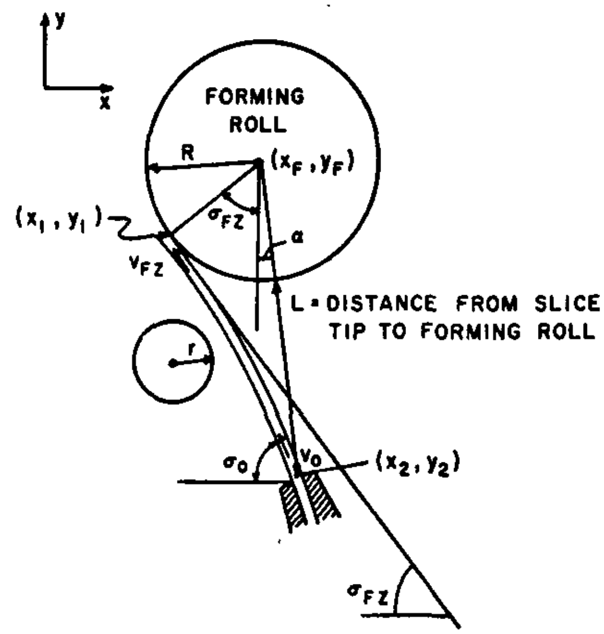

Fig. 4. Slice/forming roll jet relationships in a twin wire former.

The free jet analysis is based on the assumption of negligible air resistance (inviscid flow). Therefore, since gravity is the only force acting, the motion of the jet is governed by the vertical and horizontal components of Newton's 2nd law:

$$\frac{dV_y}{dt} = -g \qquad (18)$$

and,

$$\frac{dV_x}{dt} = 0 \qquad (19)$$

where:

V_y = vertical jet velocity
V_x = horizontal jet velocity
g = acceleration of gravity
t = time

The solution to Eq. (18) is:

$$V_y = V_{o_y} - gt \qquad (20)$$

where:

$$V_{o_y} = V_o \sin\sigma_o \qquad (21)$$

= vertical velocity component at slice

V_o = jet velocity at slice

Writing Eq. (19) as

$$\frac{d^2x}{dt^2} = 0 \quad (22)$$

where: x = particle horizontal position, and integrating gives:

$$V_x = \frac{dx}{dt} = \text{constant} \quad (23)$$

The constant horizontal velocity may be evaluated in terms of known conditions at the forming roll:

$$V_x = V_{FZ_x} = V_{FZ} \cos \sigma_{FZ} \quad (24)$$

Combining Eq. (23) and (24), and integrating gives:

$$X_2 - X = V_{FZ}(\cos \sigma_{FZ})t \quad (25)$$

Therefore, the total jet transit time from slice to former (τ) is:

$$\tau = \frac{X_2 - X_1}{V_{FZ} \cos \sigma_{FZ}} \quad (26)$$

Evaluating Eq. (20) at time $t = \tau$ gives:

$$V_{FZ} \sin \sigma_{FZ} = V_o \sin \sigma_o - g\tau \quad (27)$$

since $V_{FZ} \sin\sigma_{FZ}$ is the vertical velocity component at the forming roll.

Now, the magnitude of the velocity at the slice can be determined from:

$$V_o^2 = V_{o_x}^2 + V_{o_y}^2 \quad (28)$$

According to Eq. (24), $V_{o_x} = V_{FZ_x}$, and, by Eq. (21), $V_{o_y} = V_o \sin \sigma_o$.

Hence, using Eq. (24) and (27) one obtains:

$$V_o = \sqrt{V_{FZ}^2 + 2g\tau V_{FZ} \sin\sigma_{FZ} + (g\tau)^2} \quad (29)$$

The initial jet angle (σ_o) can next be found from Eq. (24):

$$V_{o_x} = V_o \cos\sigma_o = V_{FZ} \cos\sigma_{FZ} \quad (30)$$

or:

$$\sigma_o = \cos^{-1} (V_{FZ} \cos\sigma_{FZ}/V_o) \quad (31)$$

Next, a calculation of the length of the free jet is in order, because the tendency for a jet to become unstable increases as the length increases. If the jet is approximated as a straight line between points (x_1, y_1) and (x_1, y_2) in Fig. 4, the length is:

$$\ell_o = \sqrt{(y_1 - y_2)^2 + (x_2 - x_1)^2} \quad (32)$$

The coordinates in Eq. (32) can be derived from equations presented above and from the geometry shown in Fig. 4, assuming (x_F, y_F) is specified. However, a more exact analysis, considering the jet curvature, gives the actual length (ℓ) as:

$$\ell = \sqrt{(R + H)^2 - (R - \delta)^2} - \sqrt{R^2 - (R - \delta)^2} \quad (33)$$

with δ defined as in Fig. 3.

HEADBOX SETTINGS

Finally, the headbox pressure, position, tilt, and slice settings to produce a jet having the required initial velocity, thickness, and direction can be calculated.

The procedure *is analogous* to the one *described* in the accompanying paper (7). Knowing the initial jet angle and thickness, a combination of headbox tilt and slice settings can be calculated using the Appel equations (5,6). The headbox pressure is a function, primarily, of the jet velocity but should be corrected for friction inside the headbox and for the lowering of the apparent pressure by the velocity of the stock past the pressure sensor.

On formers where the jet travels a considerable distance vertically, upward or downward, the jet thickness may change significantly, but the quantity $h \cdot V_j$ remains constant so that the jet thickness at the vena contracta, referred to the slice position, h_o, can be used in the Appel equations:

$$h_o = h_{FZ} \cdot V_{FZ}/V_o \quad (34)$$

DISCUSSION

Although the treatment presented above has been successfully used in many practical applications, no claim can be made as to completeness or correctness. It should provide a baseline from which the papermaker may deviate to practice the more artful aspects of papermaking.

REFERENCES

1. Wahren, D., Dufva, L., and Wahlstrom, B. Mechanics of water removal in Webster-type formers. Paper Technol. and Ind. 16(4): T68-76 (April, 1975).

2. Wahren, D., Stenberg, G., and Zotterman, C. Symmetrical dewatering in Webster-type formers. Pulp Paper Can. 79(9): T276-9(Sept., 1978).

3. Andersson, I. Pilot tissue machine at KMW Development Center creates new possibilities for research on paper drying. Preprints for TAPPI 1985 Engineering Conference, 457-61.

4. Wahren, D. Initial forming processes. Pacific TAPPI Seminar, Corvallis, OR, September 11-12, 1980.

5. Appel, D. W., and Yu, Y. S. Free-streamline analyses of flow from nozzles, flow through side inlets, and flow past corners. Studies in engineering mechanics, No. 17, Center for Research in Engineering Science, University of Kansas, Lawrence, KS, March 15, 1963.

6. TAPPI TIS 014-2, TIS 014-3, TIS 014-4. All issued in 1968 and revised in 1981.

7. Wahren, D. Setting the Jet - Part 2: Fourdriniers and fourdrinier/top wire hybrids. TAPPI 1987 Twin wire Seminar.

SETTING THE JET - PART 2: FOURDRINIERS AND FOURDRINIER/TWIN WIRE HYBRIDS

Douglas Wahren
The Institute of Paper Chemistry*
Appleton, WI 54912

ABSTRACT

A method is described, and examples of its application are given for determining headbox and forming board adjustments in so-called velocity forming of paper, board, and tissue. It is built on the assumption that optimum conditions require that the suspension remaining on the forming fabric beyond the leading edge of the forming board obtains a perfectly horizontal velocity. Obstacles to and potential solutions for practical, online applications are discussed.

INTRODUCTION

Correct landing of the jet from the headbox onto the forming fabric is essential to good formation, retention, and control of sheet properties. Although information on various aspects of appropriate settings is available in the literature, no comprehensive treatment of the subject has been published.

As is demonstrated below, there is quite a large number of seemingly independent variables which have to be carefully tuned to work well in concert. In addition, slice settings have to be calculated to attain the desired process conditions. Even though an experienced operator can achieve reasonably satisfactory operating conditions by observation and manual tuning of parameters, there are too many degrees of freedom in the process to make it possible to achieve "ideal" conditions except, possibly, on single-grade machines. On high-speed paper machines, the empirical process is hampered by difficulties in obtaining a good view of the landing area because of mist and spray.

With an appropriate process description, a program can be developed to provide a consistent baseline. Such a program can be used to translate successful conditions from one operation to another by keeping constant the most important process characteristics, such as the true jet-wire differential velocity, the vertical landing velocity, the fraction of the jet deflected down for sealing purposes, etc., and by providing the operator with a list of recommended settings.

This article indicates formulas necessary for such an approach. The process description works "backward" in a literal sense in that it starts out by calculating the conditions desired at the forming board and then deduces what the headbox slice settings and other conditions have to be in order to obtain the desired conditions at the forming board.

HEDGING

The accuracy of a treatment like this depends on the accuracy of the constituent parts. In practice, it is usually difficult to measure headbox settings and geometrical relationships very accurately. Furthermore, certain aspects of papermaking, notably those dealing with the visual aspects of formation, are still an art, so there probably does not exist a unique best way or method to set up and adjust a papermaking operation. Some specific points of uncertainty are discussed in context. Hedging apart, however, the material presented below has been successfully used as a first approximation and guideline for operations ranging from kraft bag and linerboard to lightweight coating rawstock and sanitary tissue. It provides a baseline from which the papermaker can deviate to practice the more artful aspects of papermaking.

All essential elements of this treatment were summarized in the 1980 Pacific TAPPI Seminar (1), where the corresponding treatment for roll-type twin wire formers was the main subject. One of the central ideas in the present treatment is that the leading edge of the forming board should split the jet in a very particular manner so that any "jump" or "bounce" on the forming board is eliminated. Hence, the present treatment is not applicable to roll-type formers but should be applicable in principle to the initial forming zone of hybrid formers, such as the Symformer® and twin wire formers using stationary elements in the initial forming zone, e.g., the Bel Baie® types. This, however, has not been verified and would require some additional geometrical relationships to account for the nonhorizontal orientation of the former.

DEFINITIONS

Figure 1 is a definition sketch of the area being considered. The top and bottom slice lips of the headbox serve to regulate and shape the jet. The end of the inside surface of the bottom slice lip is marked by an asterisk. It is the main reference point for the location of the headbox.

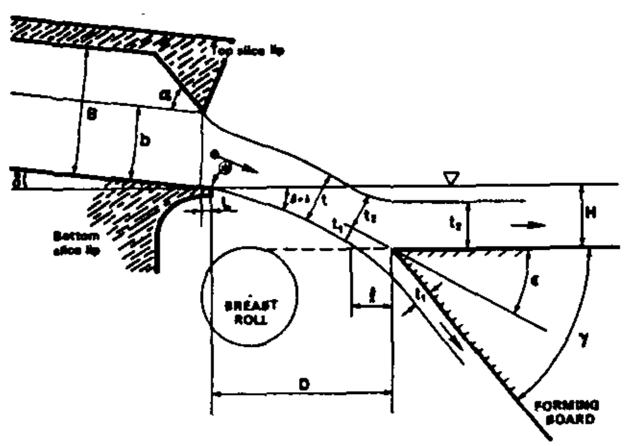

Fig. 1. Grossly exaggerated definition sketch of the headbox, slice, and forming board area. Depending on the actual values of the angle α, the channel height and the height of the "parrot beak", the sketch may represent a modern channel-type headbox with or without a "parrot beak" or an air-padded headbox.

*Present address: STORA Technology, S-79180 Falun, Sweden

As mentioned in connection with *Figure 3*, it is possible to treat most headbox designs using the descriptors defined there. The classical air-padded headbox has a 15 to 25-inch-high 90-degree beak or a 30 to 45-degree converging section which may be two to ten inches high. Many modern "hydraulic" headboxes have a more or less converging channel ending with a "parrot's beak" of modest height.

The bottom slice lip and the whole headbox may tilt (around the reference point) an angle δ from the horizontal. In practice, the tilt angle is usually fixed at zero or some other value.

The horizontal location of the top slice lip is defined by the distance L, which can be positive or negative. For traditional reasons it is designated as the extension of the bottom slice lip, although the adjustment normally is made to the top lip.

The inside angle between the top and bottom slice lips, here designated as α, is the angle used by Nelson (2) and in the Appel equations (3) which are discussed below. The vertical slice opening is conventionally designated b.

The vertical distance from the reference point on the bottom slice lip to the leading edge of the forming board is H. The most common measure used in practice is the clearance between the underside of the bottom slice lip and the forming fabric. The parameter H used here equals this clearance plus the thickness of the bottom slice lip and the thickness of the fabric. The horizontal distance, D, from the lower slice lip to the leading edge of the forming board is also indicated in the diagram. The jet lands on the forming medium a distance, l, before the leading edge of the forming board.

The jet issuing from the headbox has a thickness, t, at the *vena contracta*. A fraction of the jet, t_1/t, is deflected downward by the leading edge of the forming board. This fraction may typically be in the range 10% to 40% of the jet thickness. If it is too high, retention may suffer and the bottom of the sheet may become "sealed", making subsequent control of formation difficult. Due to the inherent roughness of the jet, the fraction deflected down must be large enough to ensure complete contact and stability of the landed jet.

Even in the absence of gravity, all the streamlines in the jet would not be perfectly straight because of the processes of redistribution of momentum and contraction. Appel's equations, discussed below, predict the angle β at the *vena contracta* in the absence of gravity. If the headbox is tilted, the tilt angle, δ is simply added to β. The effects of gravity are taken into consideration when connecting the angle ϵ between the jet and the horizontal at the location of the leading edge of the forming board to the angle β.

A fraction, t_2/t, of the jet is deflected through the angle ϵ by the forming board to attain a purely horizontal direction.

THE BASIC APPROACH: VELOCITY FORMING

This treatment deals only with so-called "velocity forming", i.e., forming without dewatering at the breast roll. It is sometimes necessary to use breastroll dewatering, but it puts stress on the forming fabric and the forming board, the position and inclination of which has to be carefully adjusted to accommodate the deflection of the fabric.

THE FORMING BOARD

In the following, the top surface of the first part of the forming board is assumed to be flat and horizontal and located to touch, but not to deflect, the underside of the forming fabric as indicated in *Figure 1*. Hence, the forming board can be described by three parameters: the horizontal and vertical distances from the slice and the angle of the leading edge of the forming board.

BASIC ASSUMPTIONS

Three basic assumptions are made:

1. The vertical velocities are so low that, for the brief initial process considered here, the forming fabric is perfectly transparent to the vertical flow.

2. A certain proportion of the jet is deflected downward by the leading edge of the forming board. After this interaction, the suspension remaining in and on the fabric obtains a perfectly horizontal velocity, i.e., the vertical component is zero.

3. All disturbing factors have been eliminated.

The first assumption may at first seem preposterous, but it is not. As it turns out, the vertical velocity component of the jet, even in very high speed operations, can usually be kept below 1 m/s (3 fps). This corresponds to the velocity achieved in a drop from a height of only 5 cm (2 inches).

Furthermore, only a small fraction of the jet thickness is involved. If 15 percent of a 12 mm (1/2 inch)-thick jet is deflected down, the total thickness (length of flow) involved is about 2 mm (1/16 inch), i.e., only a couple of times the thickness of the fabric. If only the long fiber fraction is retained in this initial process, the flow resistance of the fabric plus the retained fibers can still be very low.

The second assumption distinguishes this treatment of the situation from previous ones except (1). The assumption is a natural one to make and has been successfully used in a number of applications, but it is based only on intuitive reasoning: If the vertical velocity component is reduced to zero, then there will be no stock jump or excessive or uncontrolled drainage pressure. The process is illustrated in *Fig. 2*, which shows a jet with a downward slant being split in two by an edge. Part of the jet is deflected downward, which causes the other part to be deflected upward to conserve momentum. By judicious adjustment, the upper part of the jet can be given a purely horizontal velocity.

When using a real forming board instead of a knife edge, the jet tends to seal against, and therefore follow, the surface of the forming board. A simple experiment was performed in which small holes were drilled in a forming board close to its leading edge. It could readily be shown that atmospheric pressure at the surface of the forming board was achieved only at certain combinations of angle of attack and fraction of the jet deflected down. If too small a fraction is deflected down, a positive hydraulic pressure exists at the surface of the forming board. If too much is deflected down, the pressure at the forming board surface becomes subatmospheric. In that case, any leakage of air into the interface causes the jet to detach and "jump" up and away from the forming board.

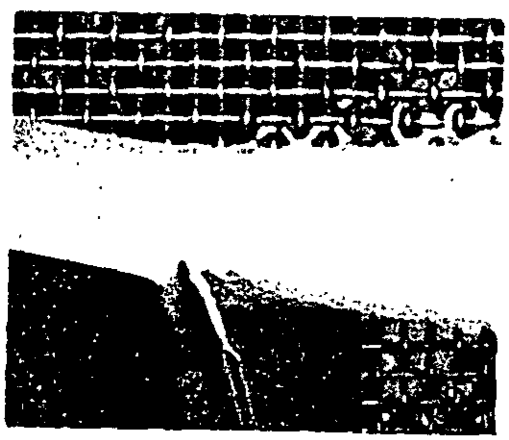

Figure 2. A free jet having a downward slant is split in two parts by a sharp edge. Appropriate adjustment of the split makes it possible to impart a purely horizontal motion to the top part of the jet.

The third assumption may not always be true, but it should be. The most common sources of severe disturbances are

A. Deformed or misaligned lower slice lip

B. Incorrect breast roll showering, allowing a high velocity boundary layer of air to follow the breast roll and to exert a pressure from below on the jet, thus deflecting the jet in an uncontrolled fashion

C. Imperfect breast roll doctor allowing water rings to form

HEADBOX ADJUSTMENTS

The above assumptions suffice to determine a range of desirable conditions at the leading edge of the forming board. Once these desirable conditions have been calculated the corresponding settings of the headbox have to be determined. Early experimental work in this area was done by Nelson (2). The mathematical treatment by Appel and Yu (3), also issued as TAPPI TIS sheets (4), is used here to calculate slice settings. The treatment could be made more general by computerizing the method of analysis developed by Attwood (5), but that has not been done.

It is clear from the experimental work reported in these references that one cannot expect extreme accuracy. Considering the experimental difficulties, it is indeed possible that the theories are better than the experiments and Appel's method has withstood the test of time. It is straightforward and easy to use even on a very small computer.

Appel's method, as used here, is limited to three cases, namely, 90, 45, and less-than-12 degree slice designs. These are three very important cases, however, which together cover most if not all current headbox designs, including the use of an add-on profile bar ("parrot's beak"). See *Figure 3* for definitions. Three variations of the slice area of headboxes are shown; many more are conceivable within the framework used here. The same notation is used in all three diagrams.

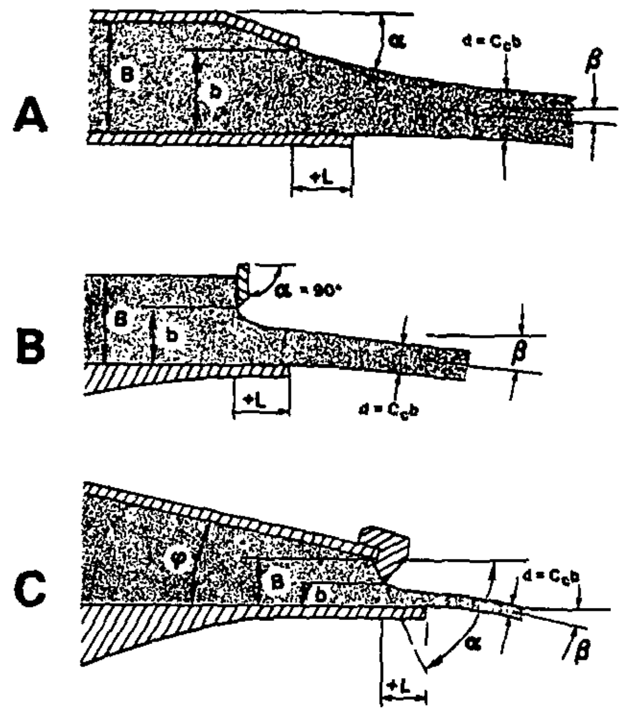

Figure 3. Headbox configurations and definitions of parameters. Only the slice and slice approach area are considered in this article. Diagram C shows a "parrot's beak" attached to the end of a channel - a configuration very widely used today.

The slice opening is b, the channel height B, and the "beak height" is B-b. The jet thickness at the *vena contracta* is $d = C_c b$ where C_c is the contraction coefficient. The projection, or extension, of the lower slice lip beyond the upper is L.

The "beak angle" is α -- whether it is a small angle in a thin channel type headbox, such as in diagram A, a 90 degree angle in a classical air-padded headbox, such as in diagram B, or the upstream side of a "parrot's beak" such as in diagram C.

The "efflux angle", β, is the angle to the lower slice lip which the jet would attain at infinity in the absence of gravity. The actual angle of the jet at the forming board, ε, is the sum of β and the influence of gravity on the jet.

The channel convergence angle, ϕ, in diagram C, is not specifically accounted for when the channel is terminated with a "parrot's beak" as in diagram C. This is of no consequence if B/b is larger than 5 and of little consequence at somewhat lower values. A tapering channel without a "parrot's beak" is covered by diagram A. Intermediate values might be inferred or cautiously interpolated. Attwood's treatment (5) might be used to advantage here but has not been attempted.

OTHER FACTORS

Among the factors which exert some influence on the process but which have been ignored are the following: friction against the air, jet break-up due to turbulence, thickness of the forming fabric, and fluid friction at and beyond the leading edge of the forming board.

No effects of edges, cross flows, misalignments, or other perils of the trade are considered.

Gravity plays an important role and its influence is always included. For the rest, the treatment summarized in the Appendix uses only standard concepts of fluid mechanics.

RESULTS

The Base Case

Sensitivity analyses were carried out around the following base conditions:

Table 1. Base conditions used for examples.

Jet thickness at forming board	10 mm	0.4 inch
Wire speed	15 m/s	2,950 fpm
Drag velocity	0.20 m/s	40 fpm
Distance, W, slice to forming board	25 cm	10 inch
Elevation, H, of slice	10 mm	0.4 inch
Forming board leading edge angle	50 deg	50 deg
Headbox tilt	0 deg	0 deg

The base case is indicated by a small circle in the following diagrams.

Headbox Elevation and Distance to Forming Board

Figure 4 illustrates the vertical velocity of the jet as it lands on the forming fabric. Parameters are the distance of the forming board from the slice and the elevation of the bottom slice lip above the forming board. The latter parameter is clearly influential. The triangles along the vertical axis and the horizontal lines in the diagram denote the velocity of free fall from the indicated heights of 5, 10, 20, and 30 mm, respectively. (A 5 mm elevation is hardly practical but illustrates the function.) It is quite clear that, if a low vertical velocity is essential, e.g., to keep the retention high, then the headbox should be located as close as is practical to the forming fabric.

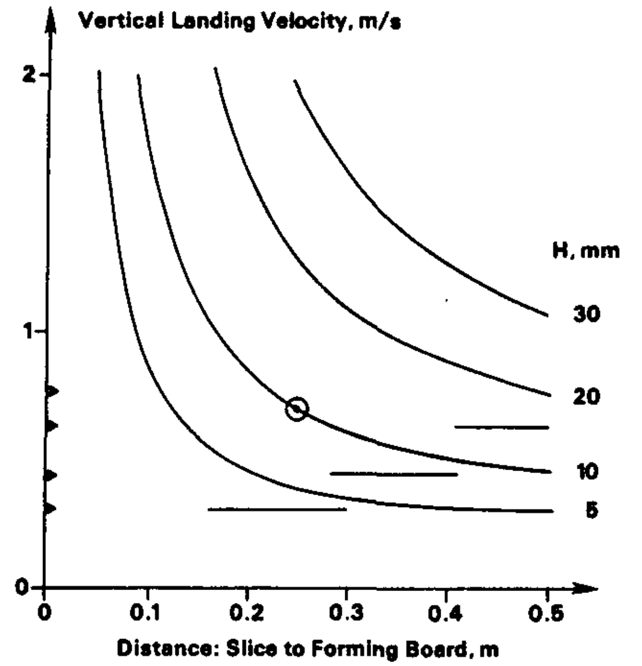

Figure 4. Jet vertical landing velocity when properly adjusted to various distances between the slice and the forming board shown for four different elevations, H, of the headbox above the forming board. Variations around the base case.

The vertical velocity component not induced by gravity is due to to the inclination, β+δ, of the jet at the slice. This downward inclination has to be reduced more the further away the forming board is located. Hence, the vertical velocity component has to be reduced more the further away the forming board is located.

Figure 5 illustrates how the fraction of the jet deflected down has to change with the distance between the slice and the forming board. Again, the influence of the elevation of the headbox is evident. The surface roughness of free jets increases with the distance travelled and with the intensity and scale of turbulence in the flow. Considering that the surface irregularities in jets from most headboxes easily reaches five or more percent of the jet thickness, it is clear that the distance between the jet and the forming board must be kept rather short.

Considering *Figures 4 and 5* together, it becomes obvious that there probably exists some limited range of headbox elevation and distance between headbox and slice which yields both a low vertical landing velocity and adequate jet deflection to ensure that no air is trapped in the suspension retained on the wire. Tilting the headbox or changing the slice configuration do not influence these relationships.

4

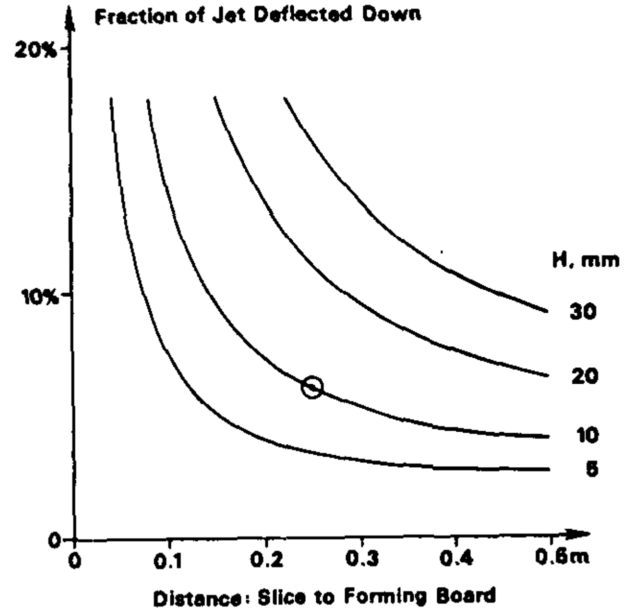

Figure 5. The fraction of the jet which has to be deflected down by the forming board depends on the distance of the forming board from the slice and on the elevation of the headbox above the forming board. Variations around the base case.

Within a reasonable range, say a factor of two, the correct *percentage* of the jet deflected down does not change significantly with the jet thickness. The slice settings, L and b, have to be adjusted, of course, and the L/b ratio has to be changed slightly (or the headbox tilted).

The Leading Edge of the Forming Board

Another lever for optimizing the conditions is provided by the angle of the leading edge of the forming board. *Figure 6* illustrates how the percentage of the jet thickness deflected down changes with the angle of the leading edge of the forming board.

The blunter the angle (up to 90 degrees plus), the more truly vertically downward is the deflection of the bottom portion of the jet and, hence, the vertical deflection of momentum. Therefore, the blunter the angle is, the smaller is the fraction of the jet which needs to be deflected in order to achieve the desired exchange of momentum to redirect the top portion of the jet to attain a purely horizontal motion. This is important in low speed operations, as will become evident in the following. In high speed operation, where air entrainment can be a problem, a relatively sharp angle should be employed to make it possible to deflect a sufficiently large portion of the jet to ensure sealing against air.

Machine Speed

So far, the jet velocity has been constant. When *the machine speed*, or rather the jet speed, is changed, virtually all other conditions have to be changed. The data in the following diagrams refer to the base case as presented in *Table 1* with the exception of the particular parameters varied and listed in each case. Hence, and as an example, when wire speed is indicated, the jet speed equals the wire speed minus the drag velocity listed in *Table 1*.*

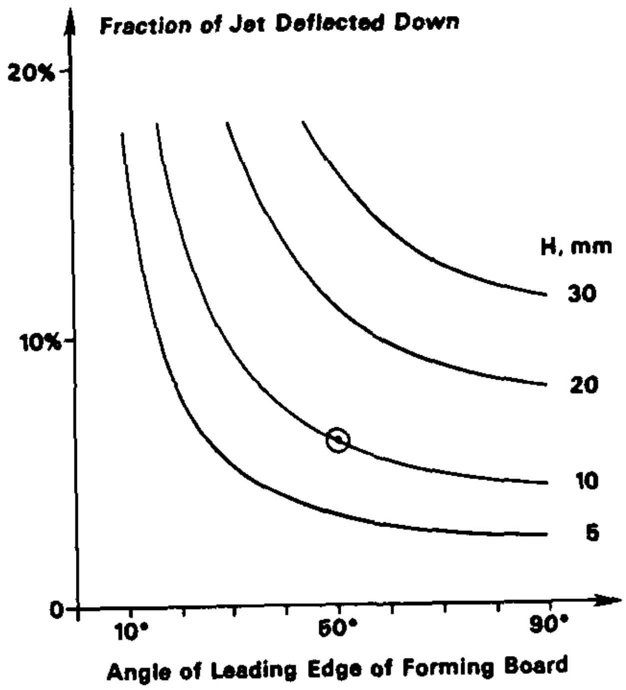

Figure 6. The fraction of the jet which has to be deflected down decreases with an increasing bluntness of the angle of the leading edge of the forming board. Variations around the base case.

Figure 7 shows how the vertical landing velocity depends on the wire speed for four different elevations of the headbox above the forming board. Again, the influence of the elevation on the landing velocity is obvious. At high wire speeds the landing velocity is almost linearly related to the wire speed, but at low speeds it levels out to a value corresponding to $\sqrt{2gH}$, where H is the elevation and g is the acceleration of gravity. These velocities are indicated as black triangles along the vertical axis.

The curves do not extend all the way to zero wire speed because, at any given elevation, H, of the headbox, there is a minimum free jet velocity required to cover the distance, D, to the forming board. The maximum distance which can be covered is given by the expression:

$$D_{max} = \frac{V_h}{g} \cdot \left(\sqrt{V_F^2 - V_h^2} - \sqrt{V_F^2 - V_h^2 - 2gH} \right) \qquad (1)$$

*It is the author's considered *opinion*, but experimentally proven fact only on roll-type twin wire formers, that it is the rush or drag **velocity, not the velocity ratio**, which governs fiber orientation.

5

where V_h is the horizontal jet velocity component at the slice and V_F is the jet velocity at the forming board.

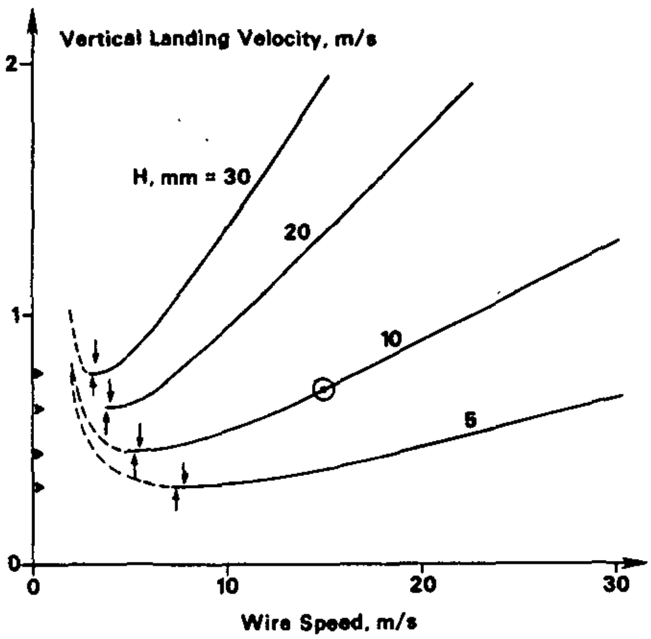

Figure 7. The jet vertical landing speed is a function of machine speed but can not drop below the velocity corresponding to the elevation of the headbox. The vertical arrows indicate approximate lower limits to usable machine speeds. These, and the dashed, "theoretical" parts of the curves are discussed in a later section. Variations around the base case.

This formula is based only on the equations of motion without friction and on the notion that the jet is linked, without friction, into a horizontal direction at the forming board. It does not, however, take into account the shape of the forming board or the fraction of the jet deflected down. In certain cases this puts further restrictions on the velocities and distances that can be used. Even as it stands, however, the formula puts some fairly stringent restrictions on how far away the forming board can be located. The maximum, practically usable free jet length is obtained when the jet exits the headbox with a very slight downward inclination.

Simple as this formula may look, for practical applications it has some nasty properties and is not used directly in the following. A reasonable approximation (within 10-15% on the "safe" side usually) for quick assessment of maximum usable distance between slice and forming board, or the minimum usable jet velocity when this distance and the elevation are given, is obtained by setting the second term within the brackets to zero, i.e.,

$$V_F^2 - V_h^2 = 2gH \tag{2}$$

This, in turn, yields expressions for the maximum distance and the minimum speed:

$$D_{max} = \sqrt{2gH(V_F^2 - gH)}/g \tag{3a}$$

$$V_{Fmin} = \sqrt{2gH + gD^2/2H} \tag{3b}$$

Estimates using the latter formula are indicated in *Figure 7* by small, vertical arrows. Arrows pointing up take into account a reasonable estimate of the distance before the forming board that the jet actually touches the wire, whereas the arrows pointing down do not. Both kinds of estimates are quite close to the "theoretical" minimum (corresponding to formula 1 but computed otherwise) indicated by the termination of the solid curves. Although these estimates are conservative in the sense that the estimated minimum velocities are slightly higher than the "theoretical" ones, they are still lower than should be used in practice. Operation close to the limiting condition causes the process to become highly sensitive to any and all disturbances, such as pressure pulsations and misalignments across the machine width. In the following diagrams, curves terminating inside the diagram indicate that limiting conditions have been reached at that point. The dashed parts of the curves indicate "theoretically possible" extensions obtainable by tilting the headbox "backward," thus imparting an upward velocity component to the jet as it exits the headbox. These ranges probably should remain "theoretical", however, and never be used in practice because analyses indicate that operations in these regimes would be highly sensitive to disturbances. The corresponding ranges are also shown in *Figure 9* but are otherwise neglected.

The data in *Figure 7* are replotted in *Figure 8*, which shows the vertical landing velocity as a function of headbox elevation for a number of different wire speeds. The limitations discussed above dictate, in this example, that wire speeds much below 5 m/s (1,000 fpm) cannot reasonably be run with a slice-to-forming board distance of 25 cm (10 inches), used as the "base case".

To complete the picture, the same data are replotted in *Figures 9 and 10.*

The Headbox

The preceding examples have dealt with the conditions (jet thickness, angle, landing point, etc.) at the leading edge of the forming board. The headbox has been characterized only with respect to location, H and D, and, implicitly, by the angle of the exiting jet, $\beta + \delta$. These are precisely what are required as entry values to use the formulas developed by Appel (3). These formulas, easily accessible through TAPPI (4), are given in parametric form but converge very rapidly and are, therefore, quick and easy to use in a computer program.*

*It should be noted that the underlying assumptions require that the "beak height", $B-b$, is, at a minimum, a significant fraction of the slice opening. Accurate data for a smooth channel are not obtained if the "beak height" is allowed to shrink to zero.

6

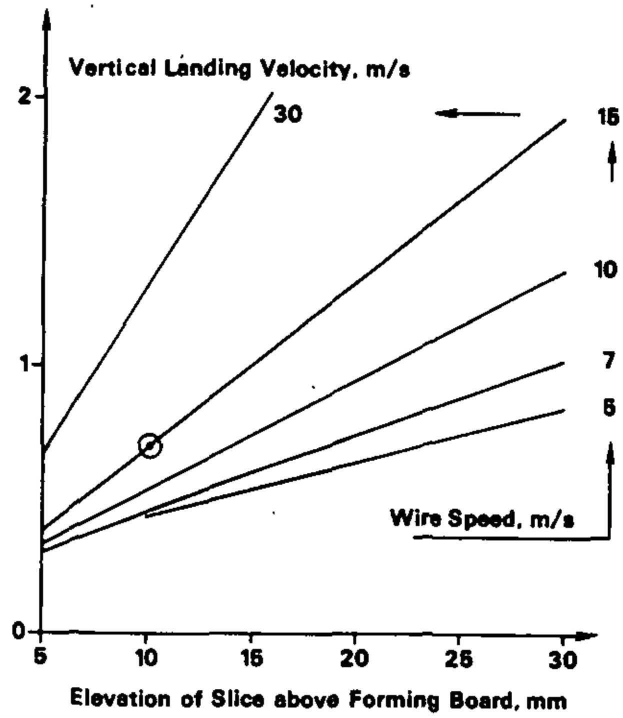

Figure 8. The jet vertical landing velocity is fairly linearly related (but not proportional) to the elevation H of the headbox. Variations around the base case.

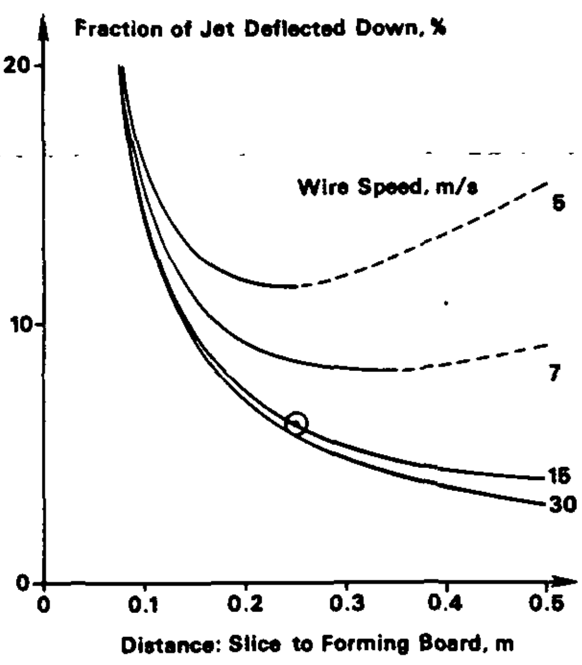

Figure 9. The fraction of the jet which has to be deflected down is a function of the distance between the headbox and the forming board and of the machine speed. Variations around the base case.

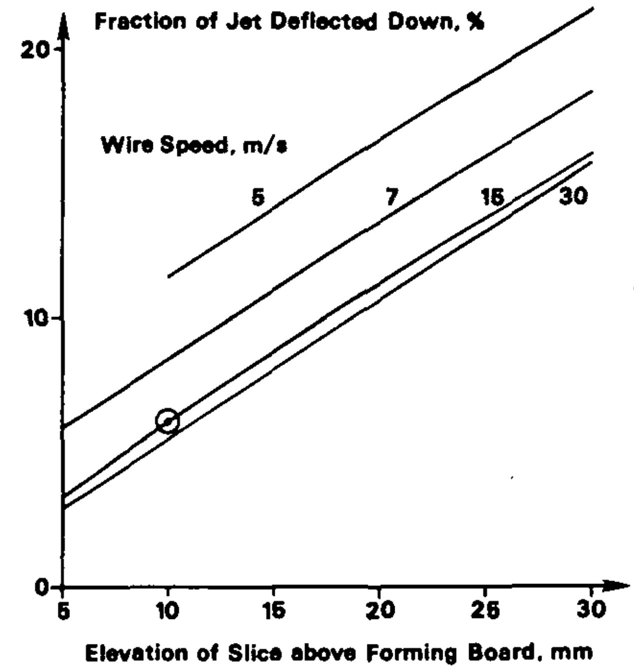

Figure 10. The fraction of the jet which has to be deflected down is a function of the elevation of the headbox and of the machine speed. Variations around the base case.

Jet Thickness

In the examples reported here, the headbox had no tilt and a 90 degree beak was used. The "beak height" was 15 mm (0.6 inch) and the jet thickness 10 mm (0.4 inch), giving an L/b ratio of 1.15. Keeping the the distance to the forming board constant and varying the jet thickness from 5 to 50 mm requires the slice opening, b, to vary from 8 to 68 mm the contraction coefficient increasing slightly (0.625 to 0.735) with the slice opening. The L/b ratio varies from 1.16 to 0.95 over the range of jet thicknesses mentioned. There is virtually no influence by the jet thickness on the vertical landing velocity.

Using a forming board with a 50 degree angle at the leading edge keeps the fraction of the jet deflected down almost independent of the slice opening. The fraction actually increases from 6 to 7.3 percent when the jet thickness is increased from 5 to 50 mm. This is unfortunate because a smaller percentage actually would suffice to keep the air out when using a thicker jet. It may be interesting to note that this results in a one-to-one correspondence between slice opening and jet thickness at the forming board, which is the same for all reasonable forming board angles. The protrusion of the lower slice lip has to be adjusted, however.

Forming Board Angle and Headbox Settings

Using other angles at the leading edge of the forming board does not influence in any way the required slice opening. Because a sharp angle of the forming board requires that more of the jet be deflected down, the lower slice lip has to be retracted more. The converse is true when using a blunter edge. The influence of the forming board angle on the vertical landing velocity is minimal; it decreases very slightly with increasing bluntness of the angle.

Headbox Tilt and *L/b* Ratio

When the convergence angle, α, in *Figures 1 and 3* is high and the *L/b* ratio is close to or below one, the exit angle of the jet is a very strong function of this ratio (2-5). Such operating conditions, therefore, become sensitive to any and all inaccuracies in the slice region. If the headbox has adequate adjustability in the machine direction of the relative positions of the upper and lower slice lips, and if it is at all possible to tilt the headbox, then a forward tilt makes it possible to use a high *L/b* ratio to promote profile stability. Using a 30 degree forming board and a tilt of 3.5 degrees, which is extreme, increases the required *L/b* from 1.1 to 2.6. This gives very good jet stability but may be excessive for a standard headbox operating on a multitude of grades.

From a theoretical point of view, a headbox tilting system could well replace MD adjustability of either or both headbox slice lips except for headboxes requiring a very extreme range of slice openings. Much would be gained from a practical point of view, as discussed later.

DISCUSSION

The task of landing the jet from the headbox on the wire appears deceptively simple, and in most cases paper will be produced whether this task is carried out in an ideal fashion or not. Correct landing of the jet can be crucial, however, to paper machine productivity and to the development of formation and other paper properties.

Most of the fundamental knowledge for determining the correct slice settings has been available for decades. Two factors have limited the applications. One is a rationale for determining a desirable jet trajectory for the approach to the forming fabric. One workable rationale is proposed here in the form of assumptions number 1 and 2.

The other limiting factor has been the computational requirements. Although the equations are simple enough, the large number of variables and the fact that practical applications require *iterative* solutions make it difficult to display detailed guidelines in a chart or handbook format. Ready access to modest computing power has changed that situation, and some examples of computed results are given in this article. The potential exists now to include computing algorithms in process guidance or control programs.

Optimizing the Jet Landing Region

Referring first to *Figures 9 and 10*, it becomes apparent that, other conditions being equal, a *larger* fraction of the jet has to be deflected down at the lower speeds. This perhaps counter-intuitive result is due to the fact that at any given elevation, *H*, (10 mm *in this case)* the vertical velocity component decreases in less than direct proportion to the machine speed (*see Figure 7*). This, in turn, makes the jet approach the forming board at a steeper angle at low speeds than it does at high speeds. The steeper approach leads to a need to deflect *more* of the jet downward in order to impart a purely horizontal motion to the rest of the jet.

At high speeds a very small fraction of the jet needs to be deflected down in order to redirect the rest of the jet. It might be desirable, however, to deflect a substantial portion of the jet to ensure against problems with entrained air. The obvious solution appears to be the use of a sharp angle of the leading edge of the forming board.

The problems with air entrainment should be less severe at low speeds than at high speeds. According to *Figures 4 and 5*, however, neither the vertical landing velocity nor the fraction of the jet required to be deflected down would decrease if the forming board were moved closer to the slice. On low speed machines it is often possible to operate at a smaller elevation of the headbox (using a *soft apron* in extreme cases) and to combine this with a move to a shorter distance between the headbox and the forming board. Such a combined move can be beneficial.

Referring to *Figure 8*, the reader is reminded that going to a larger angle of the leading edge of the forming board might also be used to minimize jet deflection at low speeds. In any event, all the required settings can be readily calculated for any number of cases and the one selected which best conforms in its fundamental process characteristics to known, successful operations.

Generic Differences Between Headboxes

Each case is different and requires different slice openings and *L/b* ratios. Using the methodology presented here for comparisons at the *same speed, thickness of the jet at the forming board, distance between headbox and forming board, and elevation of the headbox*, however, there can be virtually no difference in total pressure required to drive the jet through the slice approach region or in any one of the relations illustrated above. One is free therefore, to select the headbox design based on other criteria. Some of the finer points are the following.

Very thin channels preceding the slice cause fluid friction which has a slight influence on the pressure required to operate the headbox. Of overwhelming importance, however, is that friction and turbulence are intimately related and both relate to jet quality and fiber flocculation. If the jet quality is poor due to excessive turbulence caused by friction in a thin channel, then turbulence and friction can be decreased by the addition of a "parrot's beak" -- or increasing the height of an existing one.

A high "parrot's beak" and a steep angle (up to 90 degrees) both promote sharp contraction of the jet. This may be important for headboxes operating thin jets because a larger slice opening can be used, lessening the demand for absolute accuracy in slice adjustment, or improving the performance at constant accuracy. Headboxes operating thick jets

8

would require smaller slice openings and smaller adjustments if they were to use small angles of convergence or a modest size "parrot's beak". In neither case, however, is there any influence of the slice configuration on total pressure or flow capacity required when compared at equal conditions at the forming board.

Some Practical Concerns

There are good reasons for bringing the jet geometry under automatic control, and the knowledge base for doing it is available; however, there are other obstacles. Detailed observation of the jet landing area is often difficult, even impossible in some cases. Accurate indicators of jet landing conditions have been developed for use on some twin wire formers but are entirely lacking on fourdriniers. A few pressure sensors spread across the width of the machine and located close to the leading edge of the forming board might be a possibility.

Accurate indicators of horizontal slice settings are available and functional on very few headboxes. Actuators for horizontal slice position are frequently not functional or not functional when the headbox is pressurized. Remote control and sensing of horizontal slice settings are virtually nonexistent.

It is not easy to build or to maintain equipment for accurate horizontal slice adjustment. It is surprising that so few headboxes are equipped for precise and easy tilting. It is possible to use any number of combinations of hardware and software to facilitate tilting of the headbox around the reference point at the inside end of the lower slice lip and to provide independent elevation adjustment of that point. Such arrangements can be made very precise and, because they can be located outside the headbox, need not be as costly or difficult to maintain as if they are integral parts of the headbox. These arrangements would facilitate computer control of this critical area of the papermaking process.

Needs for Knowledge

The two basic assumptions made here, i.e., the existence of a sharp leading edge of the forming board and the transparency of the forming fabric, can be questioned, and practical modifications should be experimentally and theoretically investigated.

Note that in the theoretical treatment the leading edge of the forming board is assumed to be perfectly sharp and having the indicated angle. In practice, the leading edge of the forming board has to be slightly rounded. The minimum practical radius of curvature today appears to be around one quarter of one millimeter. This "nonideal" shape has the same effect as an increase of the angle of the leading edge. The extent of this effect might be calculated by finite element analysis, but that has not been attempted. Exploratory, small scale experiments indicate that this might be an important effect in high speed operations using thin jets.

Although the pressure drop through the forming fabric may be very low, the fabric does break up the flow and affect the interaction with the leading edge of the forming board. With multilayer types of fabrics, however, the resistance of the fabric to flow and the inertia of the water contained in the fabric might become an important consideration, not so much for the positioning of the jet as for the secondary flows which might be induced *as the jet lands on the fabric*. Such phenomena may have a direct bearing on the quality of formation achieved. This should be investigated.

REFERENCES

1. Wahren, D. Initial forming processes. Presented at the Pacific TAPPI Seminar, Corvallis, OR, Sept. 11-12, 1980.

2. Nelson, H. C. Paper machine inlet performance in relation to the fourdrinier wire. Tappi 43(4): 330(April, 1960).

3. Appel, D. W., and Yu, Y. S. Free-streamline analyses of flow from nozzles, flow through side inlets, and flow past corners. Studies in Engineering Mechanics, No. 17, Center for Research in Engineering Science, University of Kansas, Lawrence, KS, March 15, 1963.

4. TAPPI TIS 014-2, TIS 014-3, TIS 014-4. All issued 1968 and revised in 1981.

5. Attwood, D. Flow of liquids from papermaking slices. Pulp & Paper Mag. of Can., Oct., 1967, p. T-517.

APPENDIX: BASIC FORMULAS

Splitting the Jet at the Leading Edge of the Forming Board

The leading edge of the forming board splits the jet into two parts having thicknesses t_1 and t_2, respectively. The latter fraction travels horizontally after the split. The fraction deflected down, t_1/t, is selected so that the net force exerted by the forming board on the incoming jet is parallel to its direction of approach, given by the angle ε and by the x direction. This criterion also ensures that there is no net force perpendicular to the leading edge of the forming board, i.e., the y direction, which might cause flow instabilities and even mechanical vibration.

The above criterion can be expressed by writing the y-direction momentum equation for the control volume shown in *Figure 11*:

$$F_y = 0 = dV_F^2 \cdot t_2 \cdot \sin\varepsilon - dV_F^2 \cdot t_1 \cdot \sin(\gamma - \varepsilon) \qquad (4)$$

where V_F is the total jet velocity at the leading edge of the forming board. F_y is the net force on the fluid in the y-direction, and the right hand side of the equation is *the total rate of y-momentum* outflow from the control volume.

The density of the fluid is d. This equation is solved for t_1 yielding

$$t_1 = (t\sin\varepsilon)/\{\sin\varepsilon + \sin(\gamma - \varepsilon)\} \qquad (5)$$

and from Fig. 1

$$l = t_1/\sin\varepsilon$$

which completes the analysis of conditions at the leading edge of the forming board. It is of some interest to combine Equations 5 and 6:

$$l = t\{\sin\varepsilon + \sin(\gamma - \varepsilon)\} \qquad (7)$$

At normal operating conditions γ is a substantial and ε a very small angle. Equation 7 then lends support to the old rule of thumb that the jet should be landed approximately one jet thickness ahead of the forming board. Hence, that rule of thumb is qualitatively compatible with the present approach. It is not sufficient.

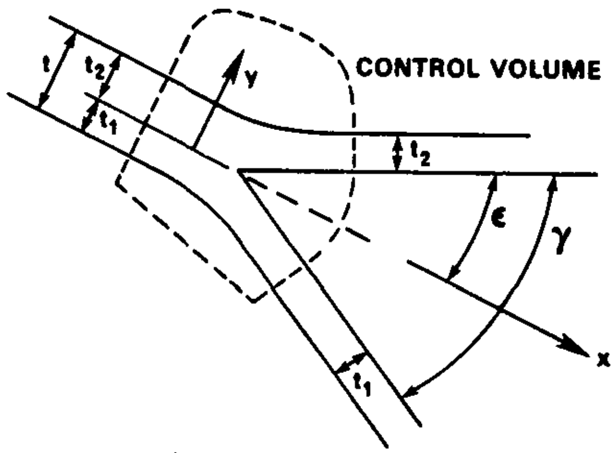

Figure 11. Momentum balance analysis at the leading edge of the forming board. The control cross section for momentum balance is enclosed by a dashed line.

The Jet Trajectory

Apart from the effects of jet contraction which are taken care of implicitly by the Appel equations, the horizontal jet velocity component, V_H, does not change in flight. The total jet velocity increases from V_0 at the slice reference point to V_F at the leading edge of the forming board:

$$V_F^2 = V_0^2 + 2gH \qquad (8)$$

where g is the acceleration of gravity. No velocity change is implied as the jet passes through the control volume. Hence, the jet velocity at the slice reference point (referred to the velocity at the *vena contracta*) can be directly calculated from Equation 8.

The time of free jet flight, T, must be the same when calculated in the horizontal and in the vertical directions:

$$H = V_{v0}T + gT^2/2 \qquad (9)$$

$$T = (D - l)/V_{h0} \qquad (10)$$

where subscripts v and h refer to the vertical and horizontal components of velocity, respectively.

The vertical velocity component is counted as positive downward. The jet efflux angle, β is obtained from

$$\tan(\beta + \delta) = V_v/V_h \qquad (11)$$

For practical, computational purposes, Equations 9-11 can be rewritten in a form that requires very few iterations for convergence:

$$\beta+\delta = \text{Arctan}\{H/D - gD/[2(V_F^2 - 2gH)\cos(\beta+\delta)]\} \qquad (12)$$

These equations suffice to determine the jet trajectory and the required efflux angle from the headbox which is adjusted to suit by tilting or by means of the protrusion of the lower slice lip, L, in *Figures 1 and 3.* If the lower slice lip is adjusted the contraction coefficient changes, which requires changing the slice opening, and so on. These calculations converge very rapidly.

If the forming board angle and the fraction of the jet deflected downward are known, then the jet angle at the leading edge of the forming board, and hence the velocity components at that point, are known and the equations can be solved directly. More commonly, however, the distance between the headbox and the forming board is known, and then a straightforward iterative computing process has to be used.

The bounds described by Equation 1 and other conditions such as the requirement that the jet angle just prior to the leading edge of the forming board must be smaller than the forming board angle itself must also be taken into account.

Headbox Pressure

Since the jet velocity at the *vena contracta*, V_c, is known, the total pressure in the channel preceding the slice is composed of the pressure required to sustain this velocity plus friction in the approach channel:

$$P_t = d \cdot V_c^2/2 + P_f \qquad (13)$$

The *frictional component* of the pressure drop through a thin, wide, converging channel having the upstream and downstream channel heights h_u and h_d, respectively, and the length, L_c, is calculated by integrating the conventional equations for pressure drop in a straight channel:

$$P_f = \frac{dV_c^2}{8} \cdot f \cdot L_c \cdot t^2 \cdot \frac{h_u + h_d}{(h_u \cdot h_d)^2} \qquad (14)$$

As before, t is the jet thickness at *vena contracta*. Since the channel walls should be hydraulically smooth and the Reynold's number is far into the turbulent regime, the friction factor, f, can be approximated very adequately by

$$f = 0.01033 - 0.002511 \cdot {}^e\text{Log}(V_c t) \qquad (15)$$

In thin channels the measured pressure, P_m, is less than the total because of the velocity of the passing flow.

$$P_m = P_t - \frac{dV_c^2}{2} \cdot \{1 - (t/h_u)^2\} \qquad (16)$$

Excepting the rather insignificant changes of the value of the second term of Equation 15, the jet velocity at the *vena contracta* is explicitly contained at only one position in the composite expression for the measured pressure. This makes it easy computationally to satisfy the frequent practical need to enter the measured pressure as an independent variable in order to compute the actual jet velocity at the forming board; a single iteration often yields the desired accuracy.

11